Journal of Solid State Chemistry 184 (2011) 729–734

Contents lists available at ScienceDirect

Journal of Solid State Chemistry

journal homepage: www.elsevier.com/locate/jssc

The effect of disorder in Ba_2YTaO_6 on the tetragonal to cubic phase transition

Qingdi Zhou [a], Brendan J. Kennedy [a,*], Justin A. Kimpton [b]

[a] School of Chemistry, The University of Sydney, Sydney, NSW 2006 Australia
[b] Australian Synchrotron, 800 Blackburn Rd, Clayton, Victoria 3168, Australia

ARTICLE INFO

Article history:
Received 28 October 2010
Accepted 6 December 2010
Available online 10 December 2010

Keywords:
Phase transition
Perovskite
Cation disorder

ABSTRACT

Synchrotron X-ray diffraction and Raman spectroscopy have been used to study the structure of the complex perovskite Ba_2YTaO_6, at temperatures down to 100 K. Where the Ta and Y cations exhibit long-range rock-salt like ordering, Ba_2YTaO_6 displays a continuous phase transition from a high temperature cubic structure, described in space group $Fm\bar{3}m$, to a tetragonal, $I4/m$, structure near 260 K. This transition is inhibited if extensive disorder and/or vacancies are/is present in the sample.

1. Introduction

Chemically substituted perovskite oxides are of considerable interest for the development of dielectric resonators and filters for use in microwave signals, as employed in contemporary mobile phones and other wireless devices. The archetypal ABO_3 perovskite structure is built from corner sharing BO_6 octahedra and possesses cubic symmetry in space group $Pm\bar{3}m$, with $a\sim4.0$ Å. In this structure, all the ions are on special positions A at $1b$ ($\frac{1}{2}$ $\frac{1}{2}$ $\frac{1}{2}$), B at $1a$ (0 0 0) and O at $3d$ ($\frac{1}{2}$00) and the range of compositions encountered is testament to the structural flexibility of the corner sharing arrangement. Indeed the majority of perovskites actually has lower than the cubic symmetry. In oxides of the form $AB_{1-x}B'_xO_3$ (where B and B' are two different cations) with $x\sim0.5$, if the size and/or charge of the two B-site cations are sufficiently different, ordering of these is often observed. In such cases, the formula is better described as $A_2BB'O_6$ [1]. This ordering is, in selected cases, sensitive to the conditions employed during the synthesis of the sample [2,3].

Traditionally diffraction methods, in particular powder X-ray diffraction, have been employed to establish the symmetry of solid oxides. Symmetry lowering in perovskites is associated with either small displacements of the anions (described as cooperative tilting of the corner sharing BO_6 octahedra) or ordering of the cations. The former can be difficult to quantify if the perovskite contains heavy atoms such as Ba ($Z=56$) or Ta ($Z=73$), whilst the latter may not be detected if the atomic number (X-ray structure factor) of the two B-site cations is similar, e.g. Y ($Z=39$) and Nb ($Z=41$) in Ba_2YNbO_6. The situation is further complicated by the tendency for numerous perovskites to exhibit high pseudo symmetry, which can be beyond the modest detection capability of many laboratory X-ray diffractometers. This has prompted some researchers to utilise different methods, and Raman spectroscopy, in particular, has enjoyed considerable success. Whereas diffraction is sensitive to long range ordering, Raman measures the local symmetry. Since the two methods do not probe the same thing, it is perhaps not unexpected that there is some conflict in the literature regarding the precise symmetry of some perovskites. This potential for conflict is compounded further by the tendency of researchers to favour a particular combination of analytical and synthetic methods.

In the present work, we report our studies of the complex perovskite Ba_2YTaO_6, the structure of which was, apparently, first reported by Layden and co-workers in 1966 [4,5]. In 1994, Zurmühlen and co-workers [6] described the dielectric and low temperature structural properties of this material. Zurmühlen et al. [6] concluded that Ba_2YTaO_6 is cubic at room temperature in the space group $Fm\bar{3}m$, but undergoes a second order transition to a tetragonal structure in $I4/m$ at 253.1 K. This transition is a consequence of out-of-phase tilting of the BO_6 octahedra around the $[0\,0\,1]_p$ axis [7]. In 2006, Lufaso and co-workers [8] demonstrated the same transition occurs upon an application of pressure with the tetragonal structure observed as the pressure was increased to above 5 GPa. Around the same time, Moreira [9], using Raman spectroscopy, concluded that the material was cubic, but that locally induced lattice distortions, arising either from stresses generated during cooling or due to the presence of some extrinsic defects, were present. The cubic structure of Ba_2YTaO_6 at room temperature has been confirmed in a number of studies [10,11].

The present work has been guided by the recent study of Ba_2YNbO_6 by Dias [2] who suggested, based on Raman measurements, that the degree of Y–Nb ordering and local symmetry is sensitive to the preparative conditions and that low temperature

* Corresponding author.
E-mail addresses: kennedyb@chem.usyd.edu.au, B.Kennedy@chem.usyd.edu.au (B.J. Kennedy).

0022-4596/$ - see front matter © 2010 Elsevier Inc. All rights reserved.
doi:10.1016/j.jssc.2010.12.011

synthetic methods favour highly distorted structures. The solid state chemistry of Ta^{5+} and Nb^{5+} is sufficiently similar to expect $BaYTaO_6$ will display similar behaviour to Ba_2YNbO_6, but the former has the advantage that there is significant X-ray contrast between Y (Z=39) and Ta (Z=73) that will allow these to be distinguished by XRD. The same cannot be claimed for Y^{3+} and Nb^{5+} (Z=41), which are isoelectronic. Raman spectroscopy is, of course, insensitive to the X-ray contrast.

2. Experimental

Polycrystalline samples of Ba_2YTaO_6 were synthesised by two methods. The first was a conventional solid state method employing $YTaO_4$ and $BaCO_3$ as the starting materials. The $YTaO_4$ precursor was first prepared using a stoichiometric amount of preheated Y_2O_3 and Ta_2O_5. After mixing, these were heated at 800 °C/12 h, and then between 1100 and 1400 °C for two weeks with periodic re-grinding in a mortar and pestle until a single phase was obtained. The pure $YTaO_4$ was then mixed with $BaCO_3$ in stoichiometric amounts and heated at 1400 °C for three days with intermittent regrinding, to yield Sample **A**. The second method (Sample **B**) used in the preparation was similar to that described by Dias and co-workers [12,13]. Stoichiometric amounts of $BaCO_3$, Y_2O_3 and Ta_2O_5 were ball milled in distilled water for 48 h. The slurry was dried and heated at 1375 °C for 8 h, then mixed with 0.4 wt% (0.84 mol%) Nb_2O_5 as a sintering aid and pelletized. The pellets were heated at 1600 °C for 4 h. A third sample (**C**) was prepared following the same protocol, except that the sintering agent was not added.

Raman spectra were recorded on Renishaw Raman inVia Reflex spectrometer, using Leica DMLM microscope with an objective of 20×. The scattered light was collected (180° backscattering geometry) along the same optical path as the incoming laser. An Ar^+ laser of 514 nm with an effective 2.6 mW power at the sample surface was used as the exciting line. A liquid N_2-cooled charge coupled device (CCD) with a grating 2400 l/mm detected the scattered light. The accumulation time for one collection was 30 s.

Synchrotron X-ray powder diffraction data were collected from 100 to 400 K for Samples **A** and **B** over the angular range $5 < 2\theta < 85°$, using X-rays of wavelength 0.82465 Å on the powder diffractometer at BL-10 beamline of the Australian Synchrotron [14]. The samples were housed in 0.3 mm diameter capillaries that were rotated during measurements. The structures were refined using the program RIETICA [15]. The peak shapes were modelled using a pseudo Voigt function and the background was estimated by interpolating up to 40 selected points.

3. Results and discussion

The room temperature Raman spectrum of the conventionally prepared Ba_2YTaO_6 Sample **A** shows four strong modes at 104, 384, 764 and 836 cm^{-1} which are, based on the work of Gregora [16], assigned to first order symmetry allowed modes of $A1_i$, E_g and F_{2g} symmetry. Several weaker features, most noticeably at 316 and 573 cm^{-1} that are either second-order features or are the result of disorder induced Raman activity are also present. It appears to be accepted [9,16–18] that the features near 316 and 573 cm^{-1}, evident in Fig. 1, cannot be used as indicators of lower symmetry. Cooling the sample below 260 K results in an increase in the background intensity and a broadening of the peak near 764 cm^{-1}, suggestive of unresolved splitting of the, cubic, E_g mode. Whereas Gregora [16] observed peaking splitting of the cubic F_{2g} mode at 109 cm^{-1}, this was not observed in our study, nor was it commented upon by Moreira [9]. In their Raman study of the series Ba_2LnTaO_6, Moreira and co-workers [9] identified three additional

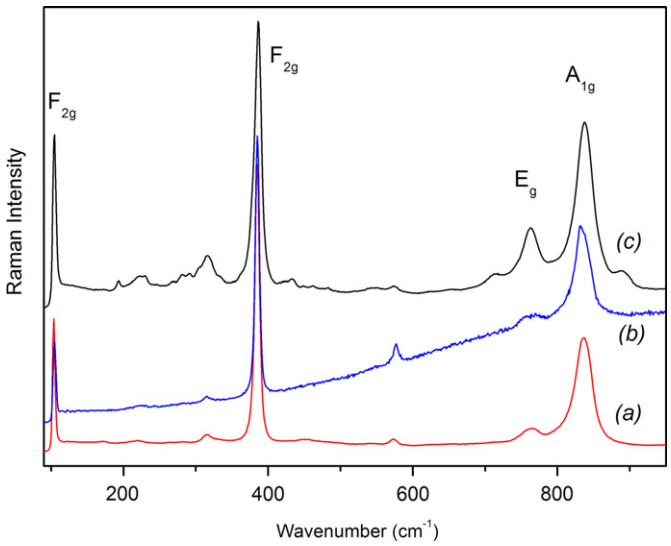

Fig. 1. Raman spectra for Ba_2YTaO_6 (a) conventionally prepared Sample **A** at 297 K, (b) conventionally prepared sample at 97 K and (c) ball-milled Sample **B** at 297 K. The spectra have been offset for clarity. The allowed Raman modes in the cubic symmetry are indicated.

bands, near 415, 550 and 720 cm^{-1} as indicative of tetragonal symmetry; although scrutiny of their published spectra suggests such modes to be very weak. Such bands were sufficiently weak in our low temperature spectra to be obscured by the high luminescence background. In brief, our Raman spectra are consistent with cubic-to-tetragonal transition upon cooling, but they do not offer conclusive evidence for this.

In addition to the six obvious features evident in Raman spectrum of the conventionally prepared sample, the spectrum of the ball-milled Sample **B** contained a number of other features, most noticeably near 711 and 430 cm^{-1} (the latter was actually best fitted as a doublet at 421 and 433 cm^{-1}) that could be assigned as arising from splitting of the cubic E_g and F_{2g} modes, respectively. Evidently there are many more bands in this spectrum than can be accounted for using cubic symmetry and it is tempting to assign tetragonal, or even lower, symmetry to this sample [2]. However, as evident from the diffraction data presented below, the sample is clearly not tetragonal; rather we propose that the additional complexity in Raman spectrum is due to local defects. Cooling this sample did not result in the appearance of any new modes in Raman spectrum; rather it simply resulted in a large increase in the background. This increase in the background effectively masks any additional features.

At this point, it is worthwhile considering the possible influence of the sintering agent. Sintering agents such as Al_2O_3 or Nb_2O_5 are commonly employed, where the preparation of dense pallets, as is necessary for the measurement of the selected physical properties of a material. Obviously, the addition of 0.4 wt% Nb_2O_5 (0.0360 g of Nb_2O_5 per 10 g of Ba_2YTaO_3) could alter the stoichiometry of the final phase; although, given similarity in the crystal chemistry of Nb and Ta, it is unlikely to result in dramatic differences, such as those seen in the present work. Analytical microscopy demonstrated an uneven distribution of the Nb throughout the sample, suggesting the Nb did not enter the main perovskite phase, but rather it segregated into the gain boundaries. Likewise no evidence was found to indicate that Zr (from the milling) was incorporated into the perovskite phase. Measurements on sample **C** prepared without the use of Nb_2O_5 were essentially identical to those presented here for the Sample **B** prepared with this additional agent.

The majority of the peaks in the synchrotron X-ray diffraction pattern from Sample **A** of Ba_2YTaO_6 prepared using conventional

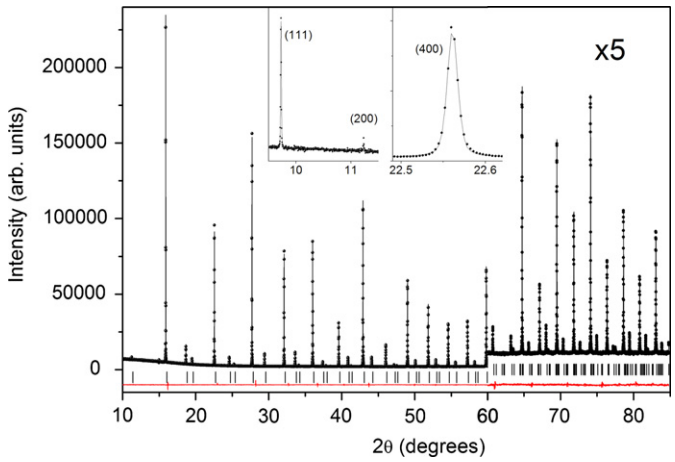

Fig. 2. Synchrotron X-ray powder diffraction profiles for the conventionally prepared Ba_2YTaO_6 sample. The solid line is the result of fitting in an $Fm\bar{3}m$. The inserts highlight the strength of the *R*-point (1 1 1) reflection near $2\theta=9.7^\circ$ and the lack of splitting of the (4 0 0) reflection near $2\theta=22.6^\circ$. Note the change in an intensity scale at $2\theta=60^\circ$, so to highlight quality of the high angle data.

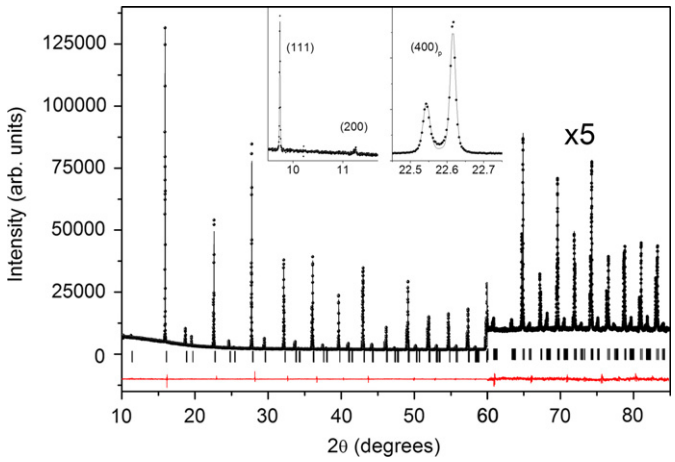

Fig. 3. Synchrotron X-ray powder diffraction profiles for the conventionally prepared Ba_2YTaO_6 sample recorded at 100 K. The solid line is the result of the fitting in an $I4/m$. The inserts highlight the strength of the *R*-point (1 1 1) reflection near $2\theta=9.7^\circ$ and the obvious splitting of the $(4\,0\,0)_p$ reflection near $2\theta=22.6^\circ$. Note the change in an intensity scale at $2\theta=60^\circ$.

solid state methods, recorded at room temperature, could be indexed to a primitive cubic structure with $a\approx4.2$ Å; there being no indication for splitting of the peaks, as evident from the insert in Fig. 2 that illustrates the (4 0 0) reflection. A small number of extremely weak peaks from an unidentified impurity phase were also present in the pattern. The pattern also included a number of weaker reflections, which were indexed as *R*-point reflections indicative of cation ordering and/or octahedral tilting. In particular, the *R*-point (1 1 1) reflection near $2\theta=9.7^\circ$ is clearly evident, and is much stronger than the (2 0 0) reflection near $2\theta=11.2^\circ$. The strength of reflections such as the (1 1 1) reflects the large X-ray scattering difference between the Y and Ta cations [1]. The presence of these *R*-point reflections requires a doubling of the primitive cell to $a=8.44152(1)$ Å and subsequently the structure was successfully refined in the space group $Fm\bar{3}m$ (tilt system $a^0a^0a^0$). The refined lattice parameter is in a reasonable agreement with previously published values that range from 8.424 to 8.435 Å [4,6,8,11].

A diffraction pattern of the conventionally prepared Ba_2YTaO_6 sample was also obtained at 100 K; the minimum temperature available using our cryostream. This pattern exhibited splitting of a number of peaks, such as the (4 0 0) reflection, shown in Fig. 3. This peak splitting was found to be consistent with $I4/m$ tetragonal symmetry (tilt system $a^0a^0c^-$) as proposed by Zurmühlen [6] and as we observed in the closely related oxide Ba_2HoTaO_6 [19]. Similarity in behaviour between Ba_2YTaO_6 and Ba_2HoTaO_6 is not unexpected, since Y^{3+} and Ho^{3+} have very similar ionic radii [20], and hence tolerance factors; and both cations can be considered as simple ionic species. $I4/m$ tetragonal symmetry features out-of-phase tilting around the *c*-axis and is often seen in double perovskites, such as Sr_2MWO_6 ($M=Ni^{2+}$ and Co^{2+}) [21,22] and Ba_2SmMoO_6 [23], and can be viewed as an intermediate between the untilted $Fm\bar{3}m$ cubic structure and lower symmetry structures [7].

Representative structural parameters and selected bond-lengths for both the cubic and tetragonal phases of Ba_2YTaO_6 are given in Tables 1 and 2, respectively. The octahedral tilting removes the equality of the Ba–O bond distances seen in the cubic structure such that there are three non-equivalent Ba–O bond-lengths in the tetragonal structure. Although the axial and equatorial bond-lengths of the YO_6 and TaO_6 octahedra are also crystallographically in-equivalent in the tetragonal phase, the refinements show (Table 2) these bond-lengths to be approximately the same. That is a regular octahedral geometry is maintained for both *B*-site cations in the tetragonal structure, despite the presence of the octahedral tilting. The average bond-lengths for all three cations do not change significantly between 100 and 400 K.

Table 1
Lattice parameters and atomic positions of cubic and tetragonal structures of the conventionally prepared Ba_2YTaO_6 sample.

Space group	$Fm\bar{3}m$	$I4/m$
Temperature (K)	300	100
a (Å)	8.44152(1)	5.95511(1)
c (Å)	$=a$	8.44829(2)
Ba	8*c* ($\frac{1}{4},\frac{1}{4},\frac{1}{4}$)	4*d* ($0\frac{1}{2},\frac{1}{4}$)
B (Å^2)	0.75(1)	0.18(1)
Y	4*a* (0 0 0)	2*a* (0 0 0)
B (Å^2)	0.41(1)	0.06(2)
Ta	4*b* ($\frac{1}{2}\,\frac{1}{2}\,\frac{1}{2}$)	2*b* ($00\frac{1}{2}$)
B (Å^2)	0.46(1)	0.10(1)
O1	24*e* (x 0 0)	4*e* (0 0 z)
x	0.2629(4)	0
z	0	0.2385(9)
B (Å^2)	1.30(4)	0.69(7)
O2		8*h* (x y 0)
x		0.2175(8)
y		0.2578(8)
B (Å^2)		0.43(6)
R_p (%)	3.27	5.2
R_{wp} (%)	4.77	6.7

The most striking feature of the synchrotron diffraction pattern of the balled milled Sample **B**, illustrated in Fig. 4, is the asymmetry of Bragg reflections towards higher angles. The asymmetry is indicative of the cubic equivalent *c*-axis being smaller than the *a*-axis rather than $c_p > a_p$ observed in the $I4/m$ structure of the conventionally prepared sample. The main Bragg reflections of this sample are broader than in the conventionally prepared sample (e.g. 0.0493(7)° vs. 0.0148(2)° for the (4 0 0) reflection). Additional reflections such as the (0 4 4) show a similar shoulder demonstrating that this is not a consequence of a lowering of symmetry.

Ting and co-workers [24,25] observed asymmetry in the diffraction patterns of the related oxide Ba_2InNbO_6, which they ascribed to

Table 2
Bond-lengths and bond valence sums (BVS) for the cubic and tetragonal structures observed in the conventionally prepared Ba_2YTaO_6 sample.

Structure	Ba–O		Y–O		Ta–O	
	Bond length (Å)	BVS	Bond length (Å)	BVS	Bond length (Å)	BVS
$Fm\bar{3}m$ 300 K	$12 \times 2.9865(1)$	1.83	$6 \times 2.219(4)$	3.45	$6 \times 2.002(4)$	4.81
$I4/m$ 100 K	$4 \times 2.867(3)$ $4 \times 2.979(2)$ $4 \times 3.106(3)$	1.90	$2 \times 2.210(5)$ $4 \times 2.216(5)$	3.50	$2 \times 2.015(5)$ $4 \times 2.008(5)$	4.70

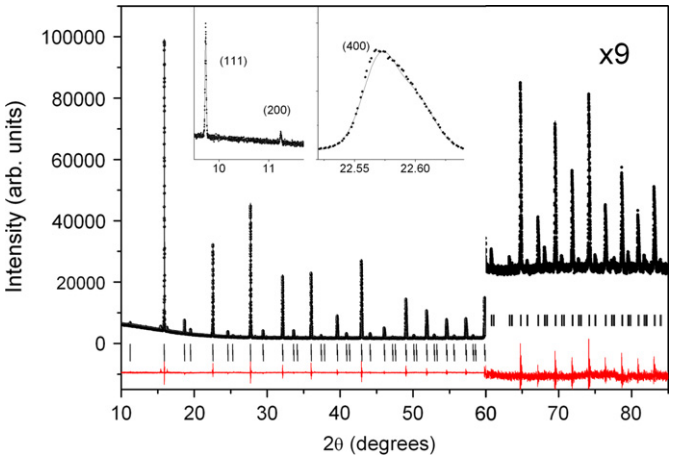

Fig. 4. Synchrotron X-ray powder diffraction profiles for the sample of Ba_2YTaO_6 prepared using a ball mill. The solid line is the result of fitting with two cubic $Fm\bar{3}m$ phases. The insert illustrates the asymmetry of the (4 0 0) reflection near $2\theta = 22.6^\circ$. Note the change in an intensity scale at $2\theta = 60^\circ$.

local distortions in the vicinity of the anti-phase boundaries arising from the stacking faults. They modelled this asymmetry by incorporating a second phase [24,25]. In order to model the asymmetry of peaks, the diffraction profile from the ball-milled Sample **B** was fitted using two cubic models, in $Fm\bar{3}m$, but allowing for disorder of the two *B*-site cations. It was not possible to estimate the precise nature of this disorder from the diffraction data due to correlation effects, but it is believed that the most likely origin of this is the fine scale stacking faults. The unit cell parameters of the two cubic phases used to fit the synchrotron diffraction pattern of the ball-milled Sample **B** (containing sintering agent) are similar, 8.43307(3) and 8.42192(3) Å, and have a relative abundance of around 2:1. These values are somewhat smaller than the value found for the conventionally prepared Sample **A**, 8.44152(1) Å. Layden and Darby have demonstrated that the non-stoichiometric materials of the type $Ba_2Y_{1-x}Ta_{1+x}O_{6-x}$ can form [5] and that the lattice parameters of these are sensitive to the precise Y:Ta ratio. Analysis of the three samples (conventionally prepared sample and the two ball-milled samples) indicate the bulk stoichiometry is as expected, suggesting the reduction in volume is related to the disorder in the sample. Synchrotron data were not obtained for Sample **C**, prepared using the ball mill, but without the sintering agent. The sensitivity of the lattice parameters to disorder has been seen in other perovskites; for example, Thomas et al. [26] predicted that the disordered structure in $La_{0.6}Sr_{0.1}TiO_3$ should have a smaller volume than the corresponding ordered material, a prediction that was experimentally verified [27]. It is not clear if the reduction in the cell volume seen for Ba_2YTaO_6 is a consequence of disorder, or if it is due to vacancies within the structure.

The diffraction data clearly shows that the brief annealing step employed after the ball-milling of the reagents is insufficient to produce a homogenous product. We note that heating the sample for 100 h at 1400 °C results in the growth of the various *R*-point

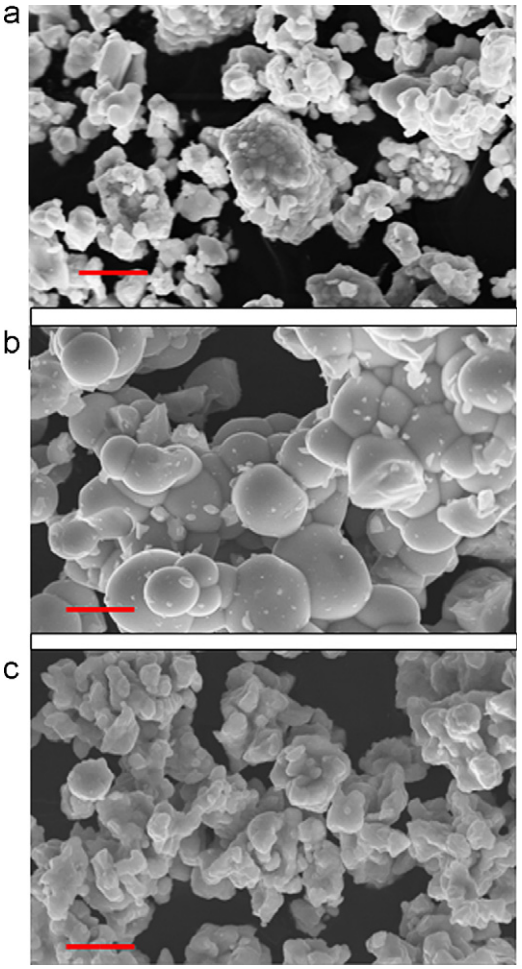

Fig. 5. SEM images of (a) Sample **B** of Ba_2YTaO_6 prepared using a ball mill band annealed for 4 h at 1600 °C, (b) the same sample annealed at 1400 °C for 100 h and (c) the conventionally prepared Sample **A**. The marker in each image shows 8 μm.

reflections demonstrating the onset of long range ordering of the Y and Ta cations. In this case, X-ray diffraction data recorded using a conventional X-ray diffractometer was well fitted to a single phase cubic model and the lattice parameter was estimated to be 8.4285 Å in a reasonable agreement with both the value estimated for the conventionally prepared Sample **A** measured under identical conditions (8.4357 Å) and previously published values that range 8.424–8.435 Å [4,6,8,11]. The in-homogeneity in the original ball-milled sample, evident in the diffraction data, accounts for changes observed in Raman spectra, illustrating the sensitivity of these types of materials to preparative conditions [27].

The evolution of the microstructure of the sample is illustrated in Fig. 5. After the initial anneal at 1600 °C for 4 h, the ball-milled Sample **B** contained a number of irregularly shaped crystallites and was clearly poorly sintered. Prolonged heating of this sample

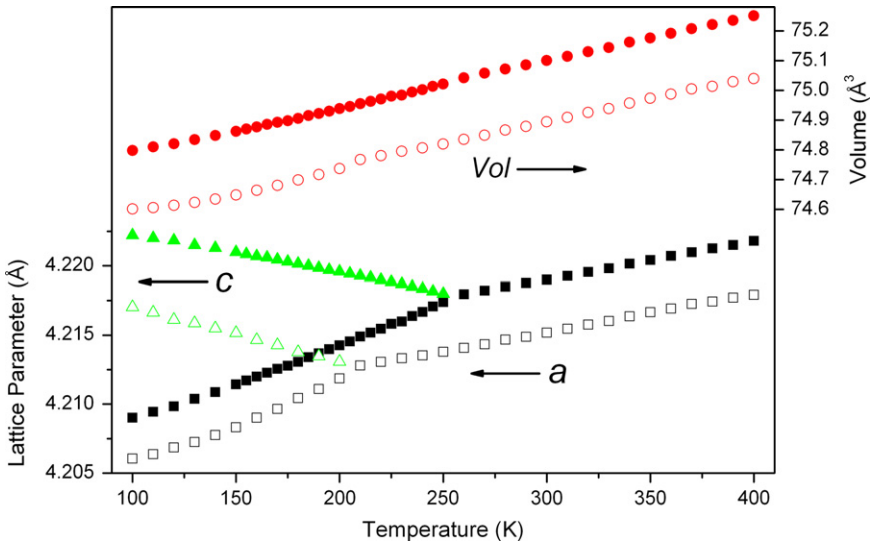

Fig. 6. Temperature dependence of the, appropriately scaled, lattice parameters and volume for conventionally prepared Sample **A** (closed symbols) and ball-mill prepared Sample **B** (open symbols) of Ba_2YTaO_6.

(~100 h at 1400 °C) resulted in the growth of the crystallites and obvious sintering of particles. At that stage, the particles are larger than those prepared using conventional solid state methods, illustrating the advantage of the ball-milled method for the preparation of dense samples.

Variable temperature X-ray diffraction data were also collected for the ball-milled Sample **B**. The diffraction pattern recorded at 100 K demonstrated the presence of a tetragonal phase, although the fit to a single $I4/m$ phase provides satisfactory R-factors (R_p=3.21 R_{wp} 4.61%), provided anisotropic broadening of the 00l type reflections was included into the fit, this model failed to reproduce the shape selected reflections. The use of a 2-phase $I4/m$ and $Fm\bar{3}m$ model rectified this problem and improved the quality of the fit (R_p=2.91 R_{wp} 3.97%). Analysis of the temperature dependence of the patterns suggests that the transition occurs at a lower (~200 K) temperature in this sample than in the conventionally prepared Sample **A** (see Fig. 6). Evidently, the disorder inhibits the transition to the tetragonal phase. Howard and co-workers showed that the tilting transition in the defect perovskite $La_{0.6}Sr_{0.1}TiO_3$ occurs at about the same temperature in both the ordered and disordered structures [27]. In $La_{0.6}Sr_{0.1}TiO_3$, the disorder is limited to the A-site cations and does not change the effective tolerance factor. The altered transition temperature in the ball-milled sample points to a change in tolerance factor in our sample, as would occur, if an appreciable amount of vacancies were present in the lattice.

Based on the laboratory X-ray diffraction data collected at a limited number of temperatures, Zurmühlen [6] concluded that Ba_2YTaO_6 underwent an improper ferroelastic second-order $I4/m$–$Fm\bar{3}m$ phase transition with a critical temperature of 253 K. To better characterise this phase transition, the structure of Ba_2YTaO_6 was investigated between 100 and 400 K; data being recorded at intervals as fine as 5 K. The phase transition between tetragonal and cubic was found to occur near 260 K. Obviously asymmetry, or peak splitting, was apparent in the (4 0 0) reflection of patterns recorded at or below 225 K. Although the (4 0 0) reflection appeared symmetrical in the data obtained at 230 K, the FWHM, 0.0227(5)°, was significantly broader than that seen at room temperature, 0.0148(2)°. Analysis shows that the width of the (4 0 0) reflection begins to broaden below 260 K reflecting the on-set of the phase transition. Fig. 6 illustrates the temperature dependence of the lattice parameters and unit cell volume. Clearly, the transition is continuous and there is no significant difference in the thermal expansion coefficients of the two phases. The transition appears to be a proper ferroelastic transition as concluded by Zurmühlen.

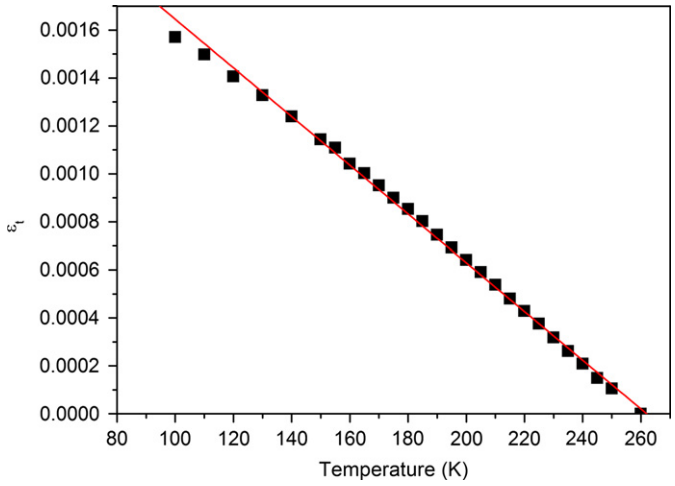

Fig. 7. Temperature dependence of the tetragonal strain in Ba_2YTaO_6 (Sample **A**). The solid line is the result of fitting to a linear expression.

The nature of the transition can be established by an examination of the temperature dependence of a suitable order parameter. In this case, the spontaneous tetragonal strain ε_t, which can be calculated from the differences in the lattice parameters as described by Carpenter [28], appears to be appropriate. A plot of ε_t against temperature, Fig. 7, is linear between 100 and 250 K. By comparison, the plot of ε_t^2 vs. T (not illustrated here) is clearly non-linear. Since the strain is proportional to Q^2 (where Q is the order parameter for a Landau-type energy expression), the linear dependence of ε_t on temperature shows the transition to be continuous and second order in nature. The deviation in strain close to the transition point is believed to reflect a limitation in accurately estimating the lattice parameters near the transition temperature, due to the reduced splitting of Bragg reflections. This is evident since a linear extrapolation of ε_t to zero strain gives a transition temperature of 262 K, slightly above the point at which any splitting or asymmetry in Bragg reflections is resolved.

4. Conclusions

The crystal structure of Ba_2YTaO_6, at temperatures down to 100 K, has been analysed by synchrotron X-ray diffraction and

Raman spectroscopy. The structure was found to be sensitive to the preparative method employed with prolonged heating necessary to induce long range ordering of the Ta and Y cations. Where such ordering was present, the sample underwent a continuous phase transition from the high temperature cubic structure in $Fm\bar{3}m$ to a tetragonal structure in $I4/m$ near 260 K. The presence of disorder in the structure appears to inhibit the tetragonal–cubic transition. Raman spectra of the disordered sample show a number of lines that are not observed in the spectra of the well annealed sample, reflecting changes in the local symmetry.

Acknowledgments

This work was, in part, performed at the powder diffraction beamline at the Australian Synchrotron. BJK acknowledges the support of the Australian Research Council for this work.

References

[1] M.T. Anderson, K.B. Greenwood, G.A. Taylor, K.R. Poeppelmeier, Progress in Solid State Chemistry 3 (1993) 197–233.
[2] A. Dias, R.G. Sa, R.L. Moreira, Journal of Raman Spectroscopy 12 (2008) 1805–1810.
[3] R.B. Macquart, Q.D. Zhou, B.J. Kennedy, Journal of Solid State Chemistry (7) (2009) 1691–1693.
[4] F.S. Galasso, G.K. Layden, D. Flinchbaugh, Journal of Chemical Physics 7 (1966) 2703.
[5] G.K. Layden, W.L. Darby, Materials Research Bulletin 4 (1966) 235–246.
[6] R. Zurmuhlen, E. Colla, D.C. Dube, J. Petzelt, I. Reaney, A. Bell, N. Setter, Journal of Applied Physics 10 (1994) 5864–5873.
[7] C.J. Howard, B.J. Kennedy, P.M. Woodward, Acta Crystallographica, Section B—Structural Science (2003) 463–471.
[8] M.W. Lufaso, R.B. Macquart, Y. Lee, T. Vogt, H.C. zur Loye, Chemical Communications 2 (2006) 168–170.
[9] R.L. Moreira, L.A. Khalam, M.T. Sebastian, A. Dias, Journal of the European Ceramic Society 8–9 (2007) 2803–2809.
[10] Y. Doi, Y. Hinatsu, Journal of Physics—Condensed Matter 19 (2001) 4191–4202.
[11] P.J. Saines, J.R. Spencer, B.J. Kennedy, M. Avdeev, Journal of Solid State Chemistry 11 (2007) 2991–3000.
[12] A. Dias, L.A. Khalam, M.T. Sebastian, R.L. Moreira, Journal of Solid State Chemistry 7 (2007) 2143–2148.
[13] A. Dias, L.A. Khalam, M.T. Sebastian, C. William, C.W.A. Paschoal, R.L. Moreira, Chemistry of Materials 1 (2006) 214–220.
[14] K.S. Wallwork, B.J. Kennedy, D. Wang, in: AIP Conference Proceedings. (2007) 879.
[15] B.A. Hunter, C.J. Howard, A Computer Program for Rietveld Analysis of X-Ray and Neutron Powder Diffraction Patterns, Lucas Heights Research Laboratories, Sydney, 1998.
[16] I. Gregora, J. Petzelt, J. Pokorny, V. Vorlicek, Z. Zikmund, Solid State Communications 11 (1995) 899–903.
[17] A. Dias, L.A. Khalam, M.T. Sebastian, M.M. Lage, F.M. Matinaga, R.L. Moreira, Chemistry of Materials 16 (2008) 5253–5259.
[18] D. Rout, G.S. Babu, V. Subramanian, V. Sivasubramanian, International Journal of Applied Ceramic Technology 5 (2008) 522–528.
[19] B.J. Kennedy, P.J. Saines, Y. Kubota, C. Minakata, H. Hano, K. Kato, M. Takata, Materials Research Bulletin 11 (2007) 1875–1880.
[20] R.D. Shannon, Acta Crystallographica, Section A SEP1 (1976) 751–767.
[21] Q.D. Zhou, B.J. Kennedy, M.M. Elcombe, Journal of Solid State Chemistry 2 (2007) 541–548.
[22] Q.D. Zhou, B.J. Kennedy, C.J. Howard, M.M. Elcombe, A.J. Studer, Chemistry of Materials 21 (2005) 5357–5365.
[23] A.C. McLaughlin, Physical Review B 13 (2008) 4.
[24] V. Ting, Y. Liu, R.L. Withers, E. Krausz, Journal of Solid State Chemistry 3 (2004) 979–986.
[25] V. Ting, Y. Liu, R.L. Withers, L. Noren, M. James, J.D.F. Gerald, Journal of Solid State Chemistry 2 (2006) 551–562.
[26] B.S. Thomas, N.A. Marks, P. Harrowell, Physical Review B 21 (2006).
[27] C.J. Howard, Z. Zhang, M.A. Carpenter, K.S. Knight, Physical Review B 5 (2007).
[28] M.A. Carpenter, Transformation Processes in Minerals, Mineralogical Society America: Washington vol. 39 (2000) 35–64.